Published in final edited form as:
Electrophoresis. 2009 October ; 30(19): 3324–3333. doi:10.1002/elps.200900317.

Amperometric Detection in Microchip Electrophoresis Devices: Effect of Electrode Material and Alignment on Analytical Performance

David J. Fischer[1,3], **Matthew K. Hulvey**[1,3], **Anne R. Regel**[2,3], and **Susan M. Lunte**[1,2,3]

[1]Department of Pharmaceutical Chemistry, University of Kansas, Lawrence, KS, USA

[2]Department of Chemistry, University of Kansas, Lawrence, KS, USA

[3]Ralph N. Adams Institute of Bioanalytical Chemistry, University of Kansas, Lawrence, KS, USA

Abstract

The fabrication and evaluation of different electrode materials and electrode alignments for microchip electrophoresis with electrochemical (EC) detection is described. The influences of electrode material, both metal and carbon-based, on sensitivity and limits of detection (LOD) were examined. In addition, the effects of working electrode alignment on analytical performance (in terms of peak shape, resolution, sensitivity, and LOD) were directly compared. Using dopamine (DA), norepinephrine (NE), and catechol (CAT) as test analytes, it was found that pyrolyzed photoresist electrodes with end-channel alignment yielded the lowest limit of detection (35 nM for DA). In addition to being easier to implement, end-channel alignment also offered better analytical performance than off-channel alignment for the detection of all three analytes. In-channel electrode alignment resulted in a 3.6-fold reduction in peak skew and reduced peak tailing by a factor of 2.1 for catechol in comparison to end-channel alignment.

Keywords

Amperometric detection; microchip electrophoresis; palladium decoupler; pyrolyzed photoresist films; carbon fiber; carbon ink

1 Introduction

A large number of microfabrication methods have been developed for the production of microchip devices since they were first reported in 1992 [1–6]. Microchip electrophoresis is among the most commonly employed formats for lab-on-chip devices and offers many potential advantages over liquid chromatography and conventional capillary electrophoresis (CE). These include decreased sample and reagent volumes, higher sample throughput, improved precision, and the possibility for disposable/portable devices. In addition, they are inexpensive and generate minimal chemical waste. The small footprint of the chip along with the ability to integrate several different processes into a single device makes this approach an attractive option for point-of-care use [7–9].

Although the miniaturized format is amenable to a large number of detection techniques, laser-induced fluorescence (LIF) and electrochemical (EC) detection are most commonly

Correspondence: Professor Susan M. Lunte, Ralph N. Adams Institute for Bioanalytical Chemistry, University of Kansas, 2030 Becker Dr., Lawrence, KS 66047, USA, Phone: +785-864-3811, Fax: +785-864-1916, slunte@ku.edu.

employed [10, 11]. LIF detection has remained very popular for microchip electrophoresis due to the relative ease of instrumental set-up and the low limits of detection that can be obtained. However, unless the analyte of interest exhibits native fluorescence, the sample must be derivatized either pre-, on-, or postcolumn prior to detection [12, 13].

Electrochemical detection is ideal for many lab-on-a-chip applications. Not only can electroactive analytes be detected without derivatization, the detector can be also be miniaturized without a loss in sensitivity. Furthermore, electrodes can be fabricated using the same photolithographic processes that are employed to produce the fluidic network. While several EC detection methods have been used for microchip electrophoresis, amperometry and conductivity are the most common [14–17]. Conductivity functions as a universal detection method that provides a response for all analytes; however, it lacks a high degree of selectivity and sensitivity [18, 19]. Amperometric detection is much more selective and sensitive than conductivity detection, but it is not universal [20]. Thus, amperometry is well suited for the detection of redox active species such as phenols, reactive oxygen (ROS) and nitrogen species (RNS), thiols, carbohydrates, and catecholamines. [9, 21–23].

One of the major challenges when using EC detection with microchip electrophoresis is decoupling the separation voltage from the detection electrode. Failure to do this properly leads to increased noise as well as probable damage to the potentiostat. The two most commonly used methods of isolating the working electrode from the separation voltage are end-channel and off-channel alignment. With end-channel alignment, the electrode is placed 5–20 μm from the end of the separation channel (Fig. 1A). This allows the separation voltage to dissipate prior to reaching the working electrode [24]. While this alignment is simple and easy to implement in microchip devices, it can lead to peak dispersion and band broadening due to the gap between the channel exit and electrode [25].

An alternative way to isolate the working electrode from the separation voltage is to use a decoupler for off-channel detection (Fig. 1B). The decoupler is placed in the separation channel ahead of the working electrode and serves as a path to ground [26–28]. Martin *et al.* described a microfabricated Pd decoupler for off-channel detection in a microchip device [29]. It has been shown that this configuration greatly reduces band broadening when compared to end channel detection.

Another approach for minimizing band broadening associated with end-channel detection is the use of an electrically isolated or “floating” potentiostat for in-channel alignment (Fig. 1C) [25, 30]. In this configuration there is no decoupler, but the working electrode can be placed directly in the separation channel because the potentiostat is not earth-grounded. A substantial improvement in peak skew and tailing was observed with this approach as compared to end-channel detection. With this configuration, the working electrode is biased by the separation voltage. Therefore, the choice of applied potential must take into account this voltage bias in order to obtain a reproducible response.

Perhaps the most important factor to consider when using EC detection is the choice of electrode material. While metal electrodes, such as Au, Pt and Pd, have been used in microfluidic devices for the detection of thiols, carbohydrates, and ROS, carbon electrodes have been the most popular choice for the detection of organic analytes, including catecholamines, phenols, and aromatic amines [9, 21–23]. In particular, carbon electrodes are ideal for the detection of catecholamines due to their large potential window, resistance to fouling, low overpotential, low background noise, and favorable electron transfer. [31–34].

The most commonly employed carbon-based electrodes are carbon fibers, pastes, and inks [35–38]. However, these three types of electrodes cannot be fabricated using standard photolithographic procedures. Therefore, their fabrication can be time-consuming and labor-intensive. An alternative carbon-based electrode material that can be fabricated *via* photolithography is pyrolyzed carbon [39, 40]. Previous work in our lab has shown that pyrolyzed photoresist film (PPF) electrodes are easily manufactured and exhibit excellent linearity and sensitivity [41]. Despite numerous reports detailing the use of carbon or metal-based electrodes, a direct comparison of the different types of materials for the detection of catecholamines has not been reported.

In this paper, we describe the fabrication and evaluation of multiple electrode materials and configurations for microchip electrophoresis with electrochemical detection. Catechol, dopamine, and norepinephrine are used as model analytes. In particular, the analytical performances of carbon fiber, carbon ink, PPF, and Pd electrodes for the detection of these analytes are directly compared. In addition, end-, off-, and in-channel electrode alignments are evaluated using Pd and carbon ink electrodes. The effect of electrode material and alignment on EC response is directly compared by evaluating the sensitivity and limits of detection (LOD). Factors such as analyte resolution, separation efficiency, and ease of fabrication and implementation are also discussed.

2 Materials and methods

2.1 Materials and reagents

The following chemicals were used as received: AZ 1518 positive photoresist and AZ 300 MIF developer (Clariant Corp., Somerville, NJ, USA); S1818 positive photoresist and Microposit 351 developer (Microchem Corp., Newton, MA, USA); SU-8 10, SU-8 2 negative photoresist and SU-8 developer (MicroChem Corp., Newton, MA, USA); 100 mm and 127 mm Si wafers (Silicon, Inc., Boise, ID, USA); Sylgard 184 (Ellsworth Adhesives, Germantown, WI, USA); dopamine (DA), catechol (CAT), norepinephrine (NE), 1 N NaOH and boric acid (BA) (Sigma-Aldrich, St. Louis, MO, USA); 2-propanol (IPA), acetone, 30% H_2O_2, H_2SO_4, HNO_3, and HCl. In addition, the following were utilized: 1 mL syringes and Pt wire (22 gauge) (Fisher Scientific, Fairlawn, New Jersey, USA); Pd (99.95% purity) and Ti (99.97% purity) targets (2 in. diameter × 0.125 in. thick; Kurt J. Lesker Co., Clairton, PA); Ti etchant (TFTN; Transene Co., Danvers, MA, USA); optical quality borosilicate glass (4 in. × 2.5 in. 0.043 in., Telic Co., Valencia, CA, USA); high temperature fused silica glass plates (4 in. × 2.5 in. × 0.085 in.; Glass Fab, Inc., Rochester, NY, USA); 33 μm diameter carbon fibers (Avco Specialty Materials, Lowell, MA, USA); conductive epoxy (ITW Chemtronics, Kennesaw, GA, USA); carbon ink and solvent thinner (Ercon Inc., Wareham, MA); colloidal silver liquid (Ted Pella, Inc., Redding, CA, USA); 0.22 μm Teflon filters (Osmonics, Inc., Minnetonka, MN, USA); 18.2 MΩ water (Millipore, Kansas City, MO, USA); quick-set epoxy and Cu wire (22 gauge; Westlake Hardware, Lawrence, KS, USA).

2.2 PDMS fabrication

The fabrication of PDMS-based microfluidic devices has been described previously [42, 43]. Detailed fabrication procedures can be found in Supporting Information section 2.2. Briefly, SU-8 10 negative photoresist (for electrophoresis channels) or SU-8 2 (for electrode channels) was spin coated on a 100 mm silicon (Si) wafer and subjected to a soft bake procedure. A negative tone transparency film was placed over the coated wafer, brought into hard contact, and exposed to a near-UV flood source. Following exposure, both wafers were post-baked, developed in SU-8 developer, rinsed with IPA, and dried under nitrogen. A 10:1 ratio of PDMS was used for all analyses, except for off-channel detection with a carbon ink

electrode. To minimize fluid leakage around the carbon ink electrode, a 20:1 ratio of PDMS was used for the electrophoresis channels. A simple "T" device containing a 3.5 cm separation channel (from the T intersection to the end of the separation channel) and 0.75 cm side arms was used for all studies reported. The width and depth of the electrophoresis microchannels were 50 μm and 14 μm, respectively.

2.3 Pyrolyzed carbon electrode fabrication

Pyrolyzed photoresist electrodes were fabricated based on a previously published technique, using two different types of positive photoresist [41]. Detailed fabrication procedures can be found in Supporting Information section 2.3. Briefly, either AZ 1518 or S1818 positive photoresist was dynamically coated on a fused silica glass plate. The coated plate was prebaked, then covered with a positive transparency film and exposed to a near-UV flood source. After exposure the plate was developed, rinsed with 18.2 MΩ water, dried under N_2, and subjected to a post-bake procedure.

A Lindberg/Blue M Three-Zone Tube Furnace (Cole-Parmer, Vernon Hills, IL, USA) was utilized for pyrolysis. The furnace was continuously flushed with nitrogen at 5 psi to provide an inert atmosphere. The temperature of the furnace started under ambient conditions and was increased at the rate of 5.5 °C/min to 925 °C, held for 1 h, and then allowed to cool to room temperature. The resultant width of the PPF electrodes was 40 μm and the height was determined with a surface profiler to be 0.6 μm.

2.4 Carbon fiber electrode fabrication

Fabrication of the PDMS carbon fiber electrode channel and placement of the carbon fiber was based on previously described work [9, 42, 44]. Detailed fabrication procedures can be found in Supporting Information section 2.4. Briefly, a 127 cm Si master containing a raised structure 33 μm wide, 33 μm high, and 3.5 cm long was fabricated in the same manner described in Section 2.2. PDMS was cast against this master to yield an electrode channel containing the same dimensions. A carbon fiber was placed directly in the electrode channel with the aid of a stereoscope. Cu wire was fixed to the substrate using quick-set epoxy, while Ag colloidal liquid (Ted Pella) was used to make electrical contact between the Cu wire and carbon fiber.

2.5 Carbon ink electrode fabrication

Two different, but related, procedures for micromolding carbon ink electrodes were utilized. When used in an end-channel configuration, the carbon ink electrode was embedded in a PDMS channel to facilitate fabrication [45, 46]. Similar to the fabrication of the carbon fiber, a channel that would house the electrode was fabricated in PDMS. The PDMS micromolding channel was aligned and sealed over the electrode channel with the aid of a stereoscope. When using a carbon ink electrode with a Pd decoupler in an off-channel configuration, a Pd contact pad was used for alignment and electrical connection. In this case, the PDMS micromolding channel was aligned so that a portion of the micromold was positioned over the Pd contact pad.

Once the electrode micromold was aligned and sealed to the electrode substrate, carbon ink electrodes were fabricated based on previously published techniques [36, 38, 45, 47, 48]. Detailed fabrication procedures can be found in Supporting Information section 2.5. Briefly, carbon ink and solvent thinner were mixed in either a 0.2% or 0.4% v/w (thinner/ink) ratio. The electrode micromold channel was primed with solvent thinner and excess solvent was removed from the reservoir. Once primed, either the 0.2% (v/w) carbon ink solution (for end-channel fabrication) or 0.4% (v/w) carbon ink solution (for off-channel fabrication) was pulled through the electrode micromold with the aid of a vacuum. When the ink solution had

filled the micromold, the entire plate was placed in an 85°C oven. After 1 h the plate was taken out of the oven, the PDMS micromold was removed, and the plate was placed in a 125°C oven for 1 h. The resulting electrode fabricated for end-channel alignment measured 50 μm wide, 8 mm long, and 1.1 μm at its tallest point from the PDMS surface. The electrode used for off-channel EC detection was 20 μm wide, 2 mm long, and 0.8 μm tall and was placed 250 μm from the Pd decoupler. This spacing had been previously optimized and was a fixed distance as determined by the fabrication of the Pd contact pad.

2.6 Palladium electrode fabrication

The Pd electrodes used for both end- and off-channel EC detection consisted of a 200 Å thick titanium (Ti) adhesion layer followed by a 2000 Å thick palladium (Pd) electrode layer deposited on a glass substrate. The Pd decoupler and electrode used for off-channel EC detection were obtained from the Nanofabrication Facility at Stanford University while the Pd electrode used for end-channel detection was fabricated in-house using a previously reported fabrication procedure [29, 38]. (***Caution!*** *Acid piranha and aqua regia solutions, which are used in this procedure, are powerful oxidizers; they should be handled with extreme care.*) Detailed fabrication procedures can be found in Supporting Information section 2.6. Briefly, glass substrates used to fabricate end-channel electrodes were cleaned in an acid piranha, rinsed thoroughly with 18.2 MΩ H_2O, and then cleaned in base piranha. The substrates were then placed into a deposition system where Ti was deposited to a thickness of ~200 Å and Pd was deposited to a thickness of ~2000 Å. Positive photoresist (S1818) was used to dynamically coat both plates to yield a photoresist thickness of 2.0–2.2 μm. The coated plate was prebaked, covered with a positive tone transparency film, and exposed to a near-UV flood source. After exposure, the plate was developed, rinsed with 18.2 MΩ water, dried under N_2, and subjected to a post-bake procedure.

The unexposed or remaining photoresist on the plate serves to protect the underlying metal from the subsequent acid-etching procedure. Pd metal was removed by immersion in aqua regia. Ti metal was removed by immersing the plate in Ti etchant (Transene) until no remaining metal could be seen. The final dimensions of the Pd electrode used for end-channel experiments measured 40 μm wide. The Pd decoupler and Pd electrode used for off-channel experiments measured 500 μm and 50 μm respectively and were separated by 250 μm.

2.7 Chip construction

Two types of microchip devices were used in these studies. An all-PDMS device was used for experiments employing a carbon fiber and carbon ink (end-channel) electrodes. A PDMS/glass hybrid device was used for all other experiments. The latter device consisted of a glass substrate, upon which the electrode was fabricated, and a layer of PDMS containing the fluid channels. The layer of PDMS containing the separation channel was aligned and reversibly sealed to the electrode plate by bringing the two substrates into conformal contact with one another. This was achieved after extensively cleaning the electrode substrate with IPA and drying with N_2. For both end-channel and off-channel EC detection using a Pd working electrode, the Pd surface was subjected to nitric acid cleaning prior to analysis. Nitric acid (6 N) was added to a PDMS reservoir and allowed to sit over the electrode for 5 min. The nitric acid was then removed from the reservoir, and the electrode was rinsed with 18.2 MΩ H_2O and dried with N_2. For end-channel EC detection, the working electrode was aligned within 5–20 μm of the exit of the separation channel (Fig. 1A). For off-channel detection, the decoupler and working electrode were placed directly in the separation channel, with the working electrode placed 20–30 μm ahead of the end of the channel exit (Fig. 1B). For experiments performed in an in-channel configuration, the electrode was also aligned 20–30 μm prior to the end of the separation channel (Fig. 1C).

2.8 Electrophoresis procedure

Electrophoresis was carried out in unmodified PDMS microchannels using a programmable Jenway Microfluidic Power Supply (Dunlow, Essex, U.K.). The electrophoresis buffer used for all data presented was 25 mM boric acid at pH 9.2. The buffer was degassed (Fisher Ultrasonic Cleaner, Fisher Scientific) and filtered with a 0.22 μm teflon filter before use. The PDMS channels were first flushed with 0.1 N NaOH for 3–5 min, then rinsed with 18.2 MΩ H_2O, and finally filled with buffer by applying a vacuum. Stock solutions (10 mM) of DA, NE, and CAT were prepared daily in 18.2 MΩ water. Samples were made prior to use by diluting with buffer. Electrophoresis was performed by applying a high voltage (+1400 V) at the buffer reservoir (B) and a fraction of this high voltage (+1200 V) at the sample reservoir (S) while the sample waste (SW) and detection reservoirs were grounded. The application of these voltages to the PDMS microchip described in section 2.2 resulted in a junction potential of 809 V and field strength of 231 V/cm. For all data presented, a gated injection method was used for introduction of the sample plug and was achieved by floating the high voltage at the buffer reservoir for the duration of the injection before returning it to +1400 V. Unless otherwise noted, an injection time of 600 ms was employed for all data presented.

2.9 Electrochemical detection

Electrochemical detection was accomplished using a CHI 802B electrochemical analyzer (CH Instruments Inc., Austin, TX, USA), a BAS Epsilon potentiostat (Bioanalytical Systems, West Lafayette, IN, USA) or a modified model 8151BP 2-Channel wireless potentiostat (Pinnacle Technology Inc., Lawrence, KS, USA) as shown in Supporting Information. Each of the three potentiostats required the use of specific data collection and analysis software. When using the CHI potentiostat, the EC response was analyzed using the built-in software package. When using the Epsilon potentiostat, signals were collected and analyzed using Chromgraph software (Bioanalytical Systems). Pinnacle Acquisition Laboratory (PAL) software was used when the Pinnacle Technology wireless potentiostat was employed. Data were collected at a sampling rate of 10 Hz when using the CHI or BAS potentiostat while a rate of 5 Hz was used when employing the Pinnacle wireless potentiostat. This was because the Pinnacle isolated potentiostat was a prototype model with a maximum sample rate of 5 Hz. The Pinnacle potentiostat was designed as a two-electrode system capable of compensating for any negative shift in half-wave potential. For experiments employing this potentiostat, a two-electrode format (working vs. Ag/AgCl reference) was used. For all other experiments a three-electrode system (working, Ag/AgCl reference, and Pt wire auxiliary) was used. For all data reported, the working electrode was set at a potential of +900 mV (vs. Ag/AgCl).

3. Results and discussion

3.1 Comparison of electrode fabrication and alignment

The growing popularity of EC detection for microchip electrophoresis has led to the development and incorporation of many different electrode materials and electrode configurations. However, in most cases, the choice of electrode material dictates the design and fabrication method for the microchip device. For example, carbon fibers must be placed manually into a channel fabricated in PDMS. This mandates the use of an all-PDMS device with an end-channel electrode alignment (Fig. 1A). Palladium decouplers can be fabricated using standard microfabrication methods, and have been shown to significantly reduce band broadening and peak skew compared to end-channel alignment. Most experiments employing a Pd decoupler employ a Pd working electrode that is deposited on the glass substrate at the same time. An exception to this is a report by Mecker *et al.* who used a Pd decoupler in conjunction with micromolded carbon ink electrodes for the detection of

catecholamines [38]. Their approach combined the benefits of off-channel EC detection and carbon-based electrodes. However, this decoupler and working electrode combination is not amenable to mass production since only the Pd decoupler is photolithographically fabricated. Alternatively, the use of in-channel alignment (Fig. 1C) further reduces band broadening but requires the use of an electrically isolated potentiostat and specialized electronics that may not be readily available.

When determining which electrode material and/or electrode alignment to use for a particular application, it is important to understand how these variables will affect analytical performance. When using end-channel alignment, it is common practice to align the electrode 5–20 μm from the channel exit. However, dramatic differences in peak height and resolution are observed with only minor changes in alignment distance. Figure 2 and Table 1 illustrate how electrode alignment can influence peak skew, resolution, and the sensitivity for a given analyte. The equations used to calculate peak skew and tailing factor can be found in Supporting Information. Figure 2A shows the electropherogram obtained using a 20 μm electrode spacing while Figure 2B shows the electropherogram obtained with 10 μm electrode spacing. As can be seen in Figure 2A, the additional 10 micron spacing leads to significant peak tailing and a considerable reduction of the resolution between DA and NE (R_S = 0.65 vs. R_S = 0.7). The inability to completely resolve NE from DA with the electrode placed 20 microns from the end of the channel (Fig. 2A) makes accurate quantitation of these two analytes difficult if not impossible. This illustrates how even small changes in the electrode alignment can directly affect the quality of analytical data.

A considerable improvement in resolution between DA and NE (R_S = 0.89) is observed when using off-channel alignment (Fig. 2C) compared to end-channel. Although the working electrode is placed directly in the channel minimizing peak dispersion due to dilution, DA and NE still exhibit a small degree of peak tailing due to the parabolic flow profile that forms between the decoupler and working electrode. This effect, as well as a significant shift in the migration time of catechol, is largely due to the change in flow dynamics from electroosmotic to hydrodynamic flow after the decoupler.

The results obtained from using an in-channel alignment are shown in Figure 2D. By placing the electrode directly in the separation channel, band broadening, peak tailing, and peak skew were significantly reduced. Even though the potentiostat had a maximum sampling rate of only 5 Hz, an increase in resolution between DA and NE (R_S = 0.91) was observed. An even larger resolution value would be expected with an increased sampling rate.

3.2 Comparison of electrode sensitivity

It is generally accepted that carbon-based materials offer superior analytical performance for EC detection of catecholamines. However, gold or platinum electrode materials have been shown to be useful for the detection of thiols and carbohydrates as well as catecholamines. Therefore, it is desirable to know exactly how the electrode material and alignment affect analytical performance. The sensitivities of the different electrodes and their alignments were determined for DA, NE, and CAT. Calibration curves were constructed over the concentration range of 0.75 to 500 μM for each analyte, electrode material, and electrode alignment. The slope of the line for each analyte (having a linear regression R^2 = 0.99 or better) was used to calculate the sensitivity. Since electrodes ranged in width from 20 to 50 μm, the sensitivity values were normalized to the largest electrode width used in the study (50 μm) to account for differences in electrode area (see Supporting Information).

Normalized sensitivity values for all three analytes using a 600 ms injection time are listed in Table 2. As expected, DA gave the largest response of the three analytes, followed by NE and CAT, regardless of the electrode material used. The carbon fiber electrode, long

considered the gold standard for carbon-based electrodes, exhibited very good sensitivity for dopamine (56.8 pA/μM). However, of all the electrode materials and alignments tested, the PPF electrode in an end-channel configuration exhibited the best sensitivity (72.0 pA/μM) for DA, a 26.7% increase in sensitivity over the carbon fiber electrode. In addition, the PPF electrode was the only electrode tested that showed a large response for sub-second injections of nanomolar concentrations of analyte. Peaks were obtained for all three analytes at a concentration of 750 nM with S/N > 3 (Fig. 3).

One surprising finding was that the sensitivity value for the end-channel Pd electrode was similar to that of the carbon fiber. Although Pd is normally thought of as an inferior electrode material for catecholamines, the sensitivity of the Pd electrode for DA was only 8% lower than that of the carbon fiber. Another unanticipated finding was that the Pd electrode exhibited significantly reduced sensitivity for all analytes when used in an off-channel detection scheme. This was unexpected because this configuration has been shown in the past to substantially reduce band broadening, leading to more efficient peaks, which should result in better sensitivity. This result was observed on multiple days with multiple electrodes (data not shown). The reason for the lower sensitivity is unclear. However, on several days, the portion of the Pd decoupler exposed to the electrophoresis channel exhibited visual signs of fouling. It is well known that catecholamines are susceptible to chemical degradation at high pH. The grounding of the separation voltage at the Pd cathode in the channel leads to the reductive electrolysis of H_2O, causing the formation of both hydrogen gas and hydroxide ions. It is possible that a high concentration of OH^- leads to analyte degradation at the surface of the palladium decoupler, reducing the amount of analyte that reaches the working electrode. Alternatively, the hydroxide ions produced at the decoupler could cause the formation of an oxide layer on the palladium working electrode, reducing the effective working electrode area and the resulting current response [49, 50].

The carbon ink electrode showed an opposite trend, with off-channel detection providing better sensitivity. One potential reason is that carbon working electrodes are less likely to be affected by large changes in pH than their counterpart metal electrodes. Another important factor is the dependence of analyte sensitivity on the carbon ink electrode fabrication process. Garcia and co-workers reported a reduction in sensitivity in EC detection with increasing carbon ink film thickness [51]. Using a carbon ink-coated gold wire, they observed that peak current (I_p) increased proportionally with the number of ink layers deposited. However, when more than 7 layers of ink were deposited (~1.0 μm total thickness), lower peak currents were obtained. The loss of signal and sensitivity was attributed to an increase in the resistance of the carbon ink film.

This phenomenon was also observed in our studies. It can be seen in Table 2 that carbon ink electrodes used in an off-channel configuration were more sensitive than those used end-channel. It has been shown that carbon ink electrodes are highly resistive and that this resistance is directly related to the amount of ink used for fabrication [52]. The electrode fabricated for end-channel use measured 50 μm wide, 8 mm long, and 16.1 μm thick, whereas the electrode used for off-channel detection was 20 μm wide, 2 mm long, and 0.8 μm thick. This is equal to a ~200-fold increase in the amount of bulk electrode material and helps to explain the attenuation of signal observed with the end-channel carbon ink electrode (Fig. 3). Furthermore, this demonstrates how seemingly small changes in fabrication can have dramatic effects on the analytical sensitivity of the resulting electrode.

3.3 Comparison of limit of detection

When evaluating the analytical performance of any detection scheme, it is important to consider not only sensitivity but also the limit of detection (LOD). Since LOD is calculated as a ratio of signal-to-noise (S/N), electrodes that do not exhibit a high degree of sensitivity

but have low background noise can still yield low theoretical limits of detection. Conversely, electrodes that exhibit high sensitivity may also have a large amount of noise, leading to higher limits of detection. The theoretical LOD for each electrode material and electrode alignment was calculated. The average noise for each concentration examined was calculated from three separate measurements of the background noise. The resulting I_p for each analyte and concentration was divided by the average noise and used to calculate LOD at S/N = 3. Representative LOD values for each electrode material and alignment were determined by averaging the resulting LOD value generated by each concentration examined. Concentration and mass LOD values for all analytes, electrode materials, and alignments can be found in Table 3. Mass detection limits were calculated using an experimentally determined injection volume of 345.6 ± 16.7 pL (data not shown).

The PPF electrode not only exhibited the best sensitivity but outperformed all other electrodes by having the lowest LOD for all three analytes (Table 3). While the pyrolyzed electrode material exhibited the largest response, it also benefited from fairly low background noise (averaging 0.85 pA peak-to-peak) as seen in Figure 3. Over the eight concentrations used in the experiment, the calculated LOD for DA averaged 73 ± 20 nM, with a best individual calculated LOD of 35 nM. Due to efficient decoupling of the separation voltage, the off-channel Pd electrode also benefited from low background noise, which resulted in a calculated LOD of 370 ± 30 nM.

Both carbon ink electrode configurations yielded calculated LODs (290 ± 90 nM for end channel; 140 ± 30 nM for off-channel) for DA that were similar to those of the carbon fiber and end-channel Pd electrode (30 ± 100 nM and 400 ± 100 nM, respectively). This finding seems to be contradictory to what one would expect, as the carbon ink electrodes were among the least sensitive electrodes tested (Table 3). However, the carbon ink electrodes exhibited the lowest noise of all the electrodes investigated (Fig. 3). Compared to more conductive materials such as Pd, the resistive electrode material leads to lower peak currents and decreased sensitivity. The increased resistivity also significantly reduces the peak-to-peak background noise (0.3 pA for carbon ink off-channel). The effects of the resultant I_p and baseline noise on the calculated LOD are illustrated in Figure 3. Despite the fact that the end-channel carbon ink electrode had the least amount of noise (Fig. 3A), the resulting I_p for a 10 μM CAT sample was smaller than that generated by a 1.0 μM or 750 nM CAT sample at a carbon fiber or PPF electrode (Fig. 3B and Fig. 3C respectively). Therefore, because LOD is calculated as a ratio of the signal (peak height) to noise, the ink electrodes had calculated LODs similar to those of other electrode materials.

The calculated LODs in Table 3 were obtained by extrapolating the response obtained for the analytes of interest in the low micromolar range to a S/N = 3. Although all of these calculated LODs are all reported to be in the nanomolar range, experimentally it was not possible to detect 1 μM DA with the carbon ink end-channel electrode as the potentiostat was not sensitive enough to detect the I_p generated at this concentration. However, dopamine was detectable at or below a 11μM concentration for all the other electrode materials and configurations.

The PPF electrode used in an end-channel alignment generated the best response for the detection of sub-micromolar concentrations of analytes. This is due to a combination of high sensitivity observed with the PPF electrodes and a small amount of background noise (0.85 nA). While the PPF electrodes were noisier than the carbon ink electrodes, the increased conductivity (reduced resistance) allowed the potentiostat to detect the change in current for lower concentration analytes. These results illustrate the importance of considering the LOD as well as the sensitivity of any particular electrode material and alignment. Understanding how both of these parameters can be affected by the electrode material or the electrode

alignment is crucial to the success of any application of EC detection for microchip electrophoresis.

3.4 In-channel EC detection

While used less frequently than end- or off-channel EC detection, in-channel detection offers many advantages. Placement of the electrode directly in the separation channel helps increase separation efficiency by limiting band broadening and peak skew. Preliminary experiments using the Pinnacle Technology wireless potentiostat illustrate the benefits of in-channel EC detection. As described earlier, the Pinnacle Technology isolated potentiostat was a prototype model that was limited to a 5 Hz sampling rate. Since its lower sampling rate restricted it from performing in a manner similar to other potentiostats used, it was not included in the direct comparison of sensitivity and LOD. However, many conclusions regarding the relationship between electrode alignment, peak shape, and analytical performance can still be made.

Using a PPF electrode in-channel, peak currents similar to those of the PPF electrode used in an end-channel configuration were observed (Fig. 2). However, since the prototype potentiostat was limited to a 5 Hz sampling rate, larger peak currents and a higher degree of sensitivity would be expected with an increased sampling rate. Alignment of the electrode directly in the separation channel mitigates the effects of band broadening and peak dispersion seen with end- or off-channel alignment. As seen in Table 1, the degree of peak skew for catechol was reduced by a factor of 2.4 over the off-channel alignment and a factor of 3.6 over the end-channel alignment. Peak tailing was also reduced by a factor of 1.9 over off-channel and 2.1 over end-channel alignment. The equations used to calculate peak skew and tailing factor can be found in Supporting Information. This reduction in band broadening led to the largest observed resolution between DA and NE ($R_S = 0.91$) compared to all other electrodes and alignments tested. Furthermore, since no decoupler is needed when using in-channel alignment, the detection scheme is less complicated than that for off-channel detection. In addition, one is not limited by the type of electrode material that can be used. This type of electrode alignment should prove very useful for many applications of microchip electrophoresis with EC detection.

4 Conclusions

The direct comparison of different electrode materials and electrode alignments for microchip electrophoresis with EC detection was described. General observations and comments on each electrode material and configuration can be found in Table 4. By comparing the influence of electrode material on EC response, it was determined that carbon-based electrode materials offered the greatest sensitivity for all three analytes. Of all materials and configurations examined, PPF electrodes used in an end-channel alignment offered the greatest sensitivity (72.0 pA/μm) and lowest calculated LOD (35 nM) for DA. It was found that, when used in an end-channel alignment, Pd electrodes exhibited an EC response similar to that of carbon fiber electrodes. This was an interesting result as carbon fiber electrodes are generally considered to exhibit superior performance over metal electrodes for the detection of organic analytes. However, lower than expected analyte sensitivity values were obtained when Pd was used for off-channel EC detection. It is postulated that this could be due to sample degradation at the decoupler that precedes the working electrode. Despite being less sensitive, comparable LOD values for this electrode were obtained due to the lower noise provided by efficient decoupling of the separation voltage from the working electrode.

Experiments using an in-channel electrode alignment significantly reduced the amount of band broadening observed in the other electrode alignment schemes. Compared to end- and

off-channel alignment, this led to a decrease in peak skew and peak tailing with increased resolution and plate number. With an improved sampling rate (>5 Hz), the authors believe that the in-channel alignment would have provided the best sensitivity and detection limits as well. This detection scheme will be investigated in future experiments involving the separation and detection of catecholamine neurotransmitters. Taken collectively, these results illustrate the dramatic effect that both electrode material and electrode alignment can have on EC response in microfluidic devices and the resulting quality of analytical data.

Supplementary Material

Refer to Web version on PubMed Central for supplementary material.

Acknowledgments

The authors thank Pinnacle Technology, Inc. for development of the electrically isolated potentiostat for in-channel analysis, Ryan Grigsby for assistance in fabrication of microchip devices, and Nancy Harmony for her assistance in the preparation of this manuscript. This research was supported by grants from the Kansas City Area Life Sciences Institute (KCALSI), the Ralph N. Adams Institute for Bioanalytical Chemistry, and National Institutes of Health (NINDS R56-NS042929-06).

References

1. Harrison DJ, Manz A, Fan Z, Ludi H, Widmer HM. Anal. Chem. 1992; 64:1926–1932.
2. Manz A, Graber N, Widmer HM. Sens. Actuators B. 1990; 1:244–248.
3. Manz A, Harrison DJ, Verpoorte E, Fettinger JC, Ludi H, Widmer HM. J. Chromatogr. 1992; 593:253–258.
4. Ohno, K-i; Tachikawa, K.; Manz, A. Electrophoresis. 2008; 29:4443–4453. [PubMed: 19035399]
5. Harrison DJ, Fluri K, Seiler K, Fan Z, Effenhauser CS, Manz A. Science. 1993; 261:895–897. [PubMed: 17783736]
6. Jacobson SC, Hergenroder R, Koutny LB, Ramsey JM. Anal. Chem. 1994; 66:1114–1118.
7. Legendre LA, Bienvenue JM, Roper MG, Ferrance JP, Landers JP. Anal. Chem. 2006; 78:1444–1451. [PubMed: 16503592]
8. Landers, JP., editor. Capillary and Microchip Electrophoresis and Associated Microtechniques. 2008.
9. Vandaveer WR IV, Pasas-Farmer SA, Fischer DJ, Frankenfeld CN, Lunte SM. Electrophoresis. 2004; 25:3528–3549. [PubMed: 15565707]
10. Pasas, SA.; Fogarty, BA.; Huynh, BH.; Lacher, NA.; Carlson, B.; Martin, RS.; Vandaveer, WR., IV, et al. Separation Methods in Microanalytical Systems. Kutter, JP.; Fintschenko, Y., editors. New York: Marcel Dekker; 2004.
11. Johnson ME, Landers JP. Electrophoresis. 2004; 25:3513–3527. [PubMed: 15565706]
12. Huynh BH, Fogarty BA, Nandi P, Lunte SM. J. Pharm. Biomed. Anal. 2006; 42:529–534. [PubMed: 16829012]
13. Li MW, Martin RS. Analyst. 2008; 133:1358–1366. [PubMed: 18810283]
14. Garcia CD, Henry CS. Bio-MEMS. 2007:265–297.
15. Castano-Alvarez M, Fernandez-Abedul MT, Costa-Garcia A. Compr. Anal. Chem. 2007; 49:827–872.
16. Martin RS. Methods Mol. Biol. 2006; 339:85–112. [PubMed: 16790869]
17. West J, Becker M, Tombrink S, Manz A. Anal. Chem. 2008; 80:4403–4419. [PubMed: 18498178]
18. Coltro WKT, da Silva JAF, Carrilho E. Electrophoresis. 2008; 29:2260–2265. [PubMed: 18446805]
19. Noblitt SD, Henry CS. Anal. Chem. (Washington, DC, U.S.). 2008; 80:7624–7630.
20. Holcomb RE, Kraly JR, Henry CS. Analyst. 2009; 134:486–492. [PubMed: 19238284]

21. Kuhnline CD, Gangel MG, Hulvey MK, Martin RS. Analyst. 2006; 131:202–207. [PubMed: 16440083]
22. Vickers JA, Henry CS. Electrophoresis. 2005; 26:4641–4647. [PubMed: 16294295]
23. Amatore C, Arbault S, Bouton C, Drapier J-C, Ghandour H, Koh ACW. ChemBioChem. 2008; 9:1472–1480. [PubMed: 18491327]
24. Huang X, Zare RN, Sloss S, Ewing AG. Anal. Chem. 1991; 63:189–192. [PubMed: 1812795]
25. Martin RS, Ratzlaff KL, Huynh BH, Lunte SM. Anal. Chem. 2002; 74:1136–1143. [PubMed: 11924975]
26. Wallingford RA, Ewing AG. Anal Chem. 1987; 59:1762–1766. [PubMed: 3631501]
27. Osbourn DM, Lunte CE. Anal. Chem. 2003; 75:2710–2714. [PubMed: 12948140]
28. Wu C-C, Wu R-G, Huang J-G, Lin Y-C, Chang H-C. Anal. Chem. 2003; 75:947–952. [PubMed: 12622389]
29. Lacher NA, Lunte SM, Martin RS. Anal. Chem. 2004; 76:2482–2491. [PubMed: 15117187]
30. Hebert NE, Kuhr WG, Brazill SA. Electrophoresis. 2002; 23:3750–3759. [PubMed: 12432538]
31. Lacher NA, Garrison KE, Martin RS, Lunte SM. Electrophoresis. 2001; 22:2526–2536. [PubMed: 11519957]
32. McCreery, RL.; Cline, KK. Laboratory Techniques in Electroanalytical Chemistry. Kissinger, PT.; Heineman, WR., editors. New York: Marcel Dekker; 1996. p. 293-332.
33. Zachek MK, Hermans A, Wightman RM, McCarty GS. J. Electroanal. Chem. 2008; 614:113–120.
34. Chesney, DJ. Laboratory Techniques in Electroanalytical Chemistry, 2nd Edition. Edited by Peter T. Kissinger (Purdue University) and William R. Heineman (University of Cincinnati). 1996.
35. Gawron AJ, Martin RS, Lunte SM. Electrophoresis. 2001; 22:242–248. [PubMed: 11288891]
36. Kovarik ML, Torrence NJ, Spence DM, Martin RS. Analyst. 2004; 129:400–405. [PubMed: 15116230]
37. Liu C, Li X, Lu G. Huaxue Yanjiu Yu Yingyong. 2005; 17:443–447.
38. Mecker LC, Martin RS. Electrophoresis. 2006; 27:5032–5042. [PubMed: 17096314]
39. Kim J, Song X, Kinoshita K, Madou M, White R. J. Electrochem. Soc. 1998; 145:2314–2319.
40. Ranganathan S, McCreery R, Majji SM, Madou M. J. Electrochem. Soc. 2000; 147:277–282.
41. Fischer DJ, Vandaveer WR IV, Grigsby RJ, Lunte SM. Electroanalysis. 2005; 17:1153–1159.
42. Martin RS, Gawron AJ, Lunte SM, Henry CS. Anal. Chem. 2000; 72:3196–3202. [PubMed: 10939387]
43. Madou, MJ. Fundamentals of microfabrication: The science of minaturization. CRC Press; 2002.
44. McDonald JC, Duffy DC, Anderson JR, Chiu DT, Wu H, Schueller OJA, Whitesides GM. Electrophoresis. 2000; 21:27–40. [PubMed: 10634468]
45. Hulvey MK, Genes LI, Spence DM, Martin RS. Analyst. 2007; 132:1246–1253. [PubMed: 18318286]
46. Hulvey MK, Martin RS. Anal. Bioanal. Chem. 2009; 393:599–605. [PubMed: 18989663]
47. Mecker LC, Martin RS. Anal. Chem. 2008; 80:9257–9264. [PubMed: 19551945]
48. Spence DM, Torrence NJ, Kovarik ML, Martin RS. Analyst. 2004; 129:995–1000. [PubMed: 15508026]
49. Genesca J, Victori L. Rev. Coat. Corros. 1981; 4:325–348.
50. Burke LD, Roche MBC. J. Electroanal. Chem. Interfacial Electrochem. 1985; 186:139–154.
51. Ding Y, Ayon A, Garcia CD. Anal. Chim. Acta. 2007; 584:244–251. [PubMed: 17386611]
52. Grennan K, Killard AJ, Smyth MR. Electroanalysis. 2001; 13:745–750.

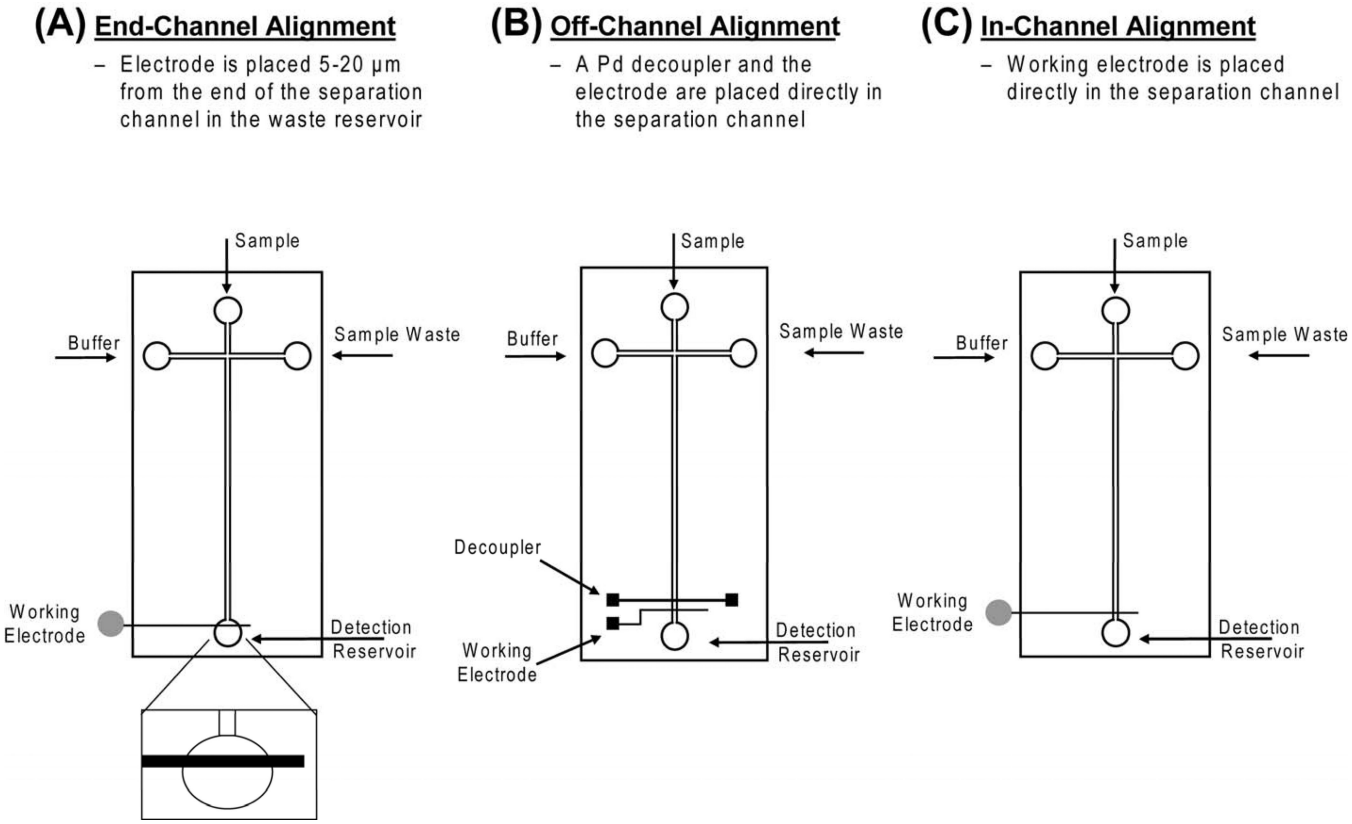

Figure 1.

Schematic of different electrode alignments for microchip electrophoresis with EC detection: (A) end-channel electrode alignment, (B) off-channel electrode alignment, (C) in-channel electrode alignment. In-channel alignment is possible only when using an electrically isolated potentiostat.

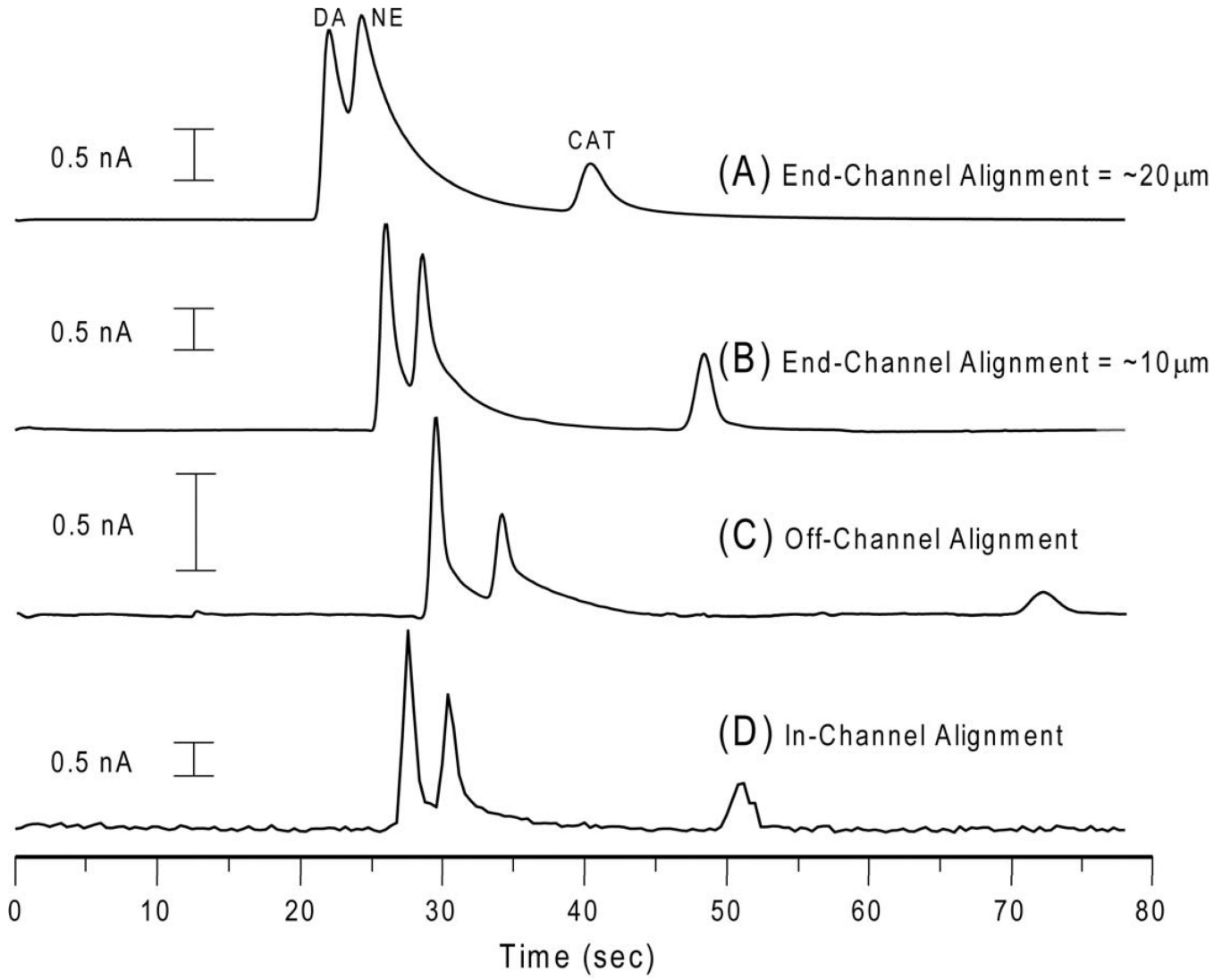

Figure 2.

Effect of electrode alignment on resolution and peak shape. (A) PPF electrode with end-channel alignment ~20 μm from end of the separation channel; (B) carbon fiber electrode with end-channel alignment ~10 μm from the end of the separation channel; (C) Pd electrode and decoupler with off-channel alignment; (D) PPF electrode with in-channel alignment. Separation conditions: 25 mM boric acid, pH 9.2; applied voltage +1400 V to B, +1200 V to S; 400 ms gated injection; E_{app} = +900 mV *vs.* Ag/AgCl. All analytes were 100 μM.

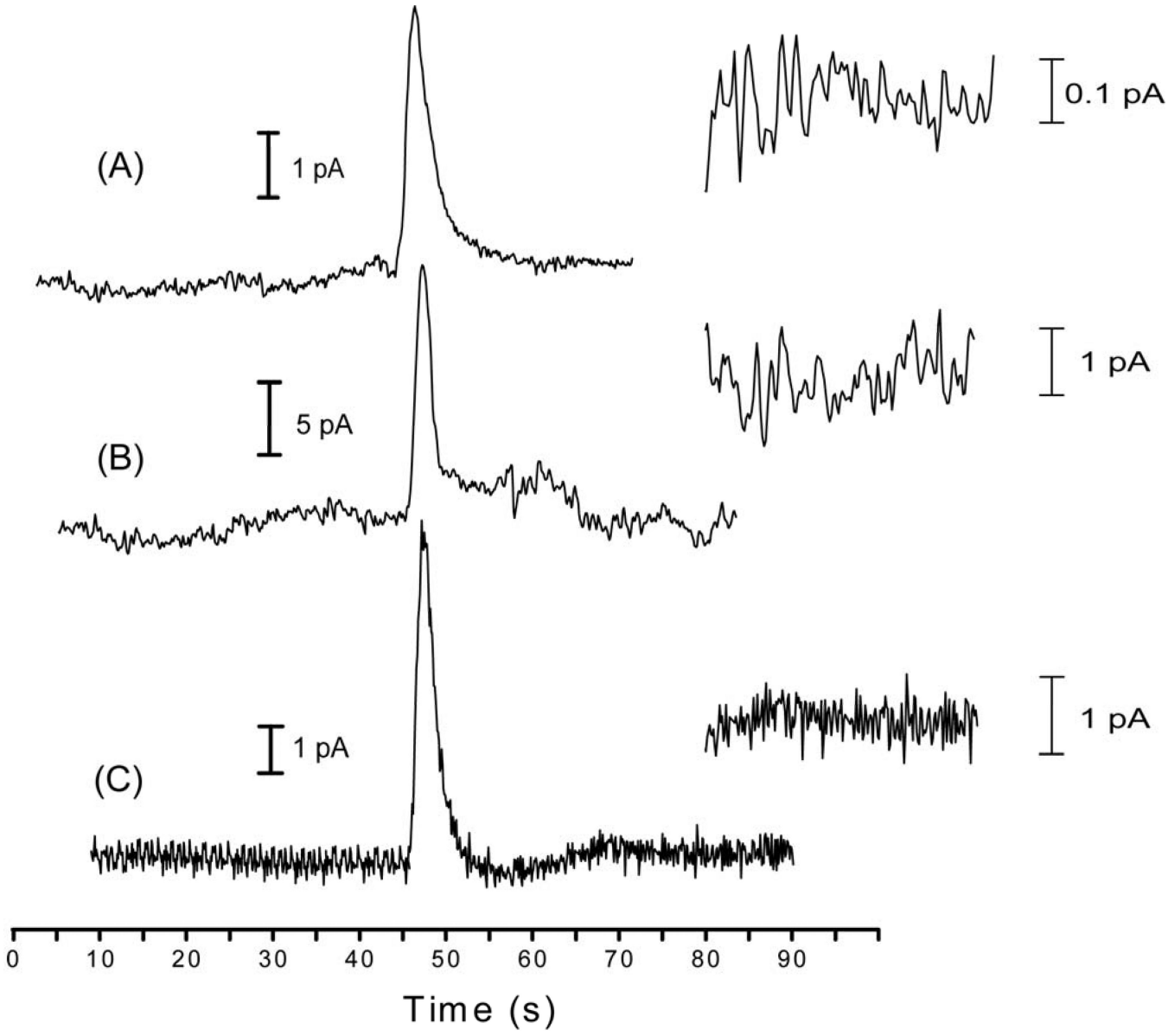

Figure 3.
EC response of CAT at three different end-channel carbon electrodes. (A) 10 μM CAT at a carbon ink electrode; (B) 1.0 μM CAT at a carbon fiber electrode; (C) 750 nM CAT at a PPF electrode. An expanded view of the baseline noise is inset for each electropherogram.

Table 1

Effect of Alignment on Resolution and Peak Shape*

	Rs[1]	N[2]	H[2](μm)	Skew[2]	Tailing Factor[2]
PPF End - Channel	0.65	379.0	92.3	3.6	2.3
Carbon Fiber End - Channel	0.70	1195	29.3	2.7	1.9
Palladium Off - Channel	0.89	3327	10.5	1.8	1.4
PPF In - Channel	0.91	5351	6.54	0.75	0.88

[1]Determined using DA and NE peaks

[2]Determined using CAT peak

*Calculated from Figure 2

Table 2

Normalized Sensitivity (pA/μM) for All Analytes

	Dopamine	Norepinephrine	Catechol
PPF End - Channel	72 ± 2	44 ± 1	15.03 ± 0.04
Carbon Fiber End - Channel	56.8 ± 0.1	45.1 ± 0.9	18.3 ± 0.3
Palladium End - Channel	52.5 ± 0.3	41.1 ± 0.3	10.67 ± 0.09
Palladium Off - Channel	12 ± 1	7.4 ± 0.2	0.84 ± 0.01
Carbon Ink Off - Channel	20.2 ± 0.2	8.2 ± 0.1	5.22 ± 0.06
Carbon Ink End - Channel	4.34 ± 0.02	2.28 ± 0.02	0.418 ± 0.003

Table 3

Concentration (nM) and Mass (amol) LOD Values for All Analytes

	Dopamine		Norepinephrine		Catechol	
	Concentration (nM)	**Mass (amol)**	**Concentration (nM)**	**Mass (amol)**	**Concentration (nM)**	**Mass (amol)**
PPF End - Channel	73 ± 20	25 ± 8	110 ± 20	37 ± 8	200 ± 80	70 ± 30
Carbon Fiber End - Channel	300 ± 100	110 ± 50	300 ± 100	120 ± 40	700 ± 100	250 ± 40
Palladium End - Channel	400 ± 100	130 ± 50	500 ± 200	160 ± 60	1800 ± 600	600 ± 200
Palladium Off - Channel	370 ± 30	130 ± 10	680 ± 30	240 ± 10	4000 ± 1000	1400 ± 500
Carbon Ink Off - Channel	140 ± 30	49 ± 9	400 ± 100	140 ± 40	500 ± 200	170 ± 60
Carbon Ink End - Channel	290 ± 90	100 ± 30	500 ± 100	170 ± 40	3000 ± 1000	1000 ± 300

Table 4

Qualitative Assessment of Microchip Performance

	Analytical Parameters			Fabrication Procedure			Remarks
	Sensitivity[1]	Limit of Detection[2]	Noise[3]	Process	Cost	Use of Hazardous Chemicals[4]	
PPF End - Channel	Best	Best	Low	Simplest	Moderate	No	Requires fused silica substrate; high temperature furnace
Carbon Fiber End - Channel	Good	Fair	Fair	Simple	Inexpensive	No	Requires skill to embed carbon fiber into PDMS substrate
Palladium End - Channel	Good	Fair	High	Complex	Expensive	Yes	Deposition system required; use of expensive or rare metals
Palladium Off - Channel	Poor	Fair	Fair	Complex	Expensive	Yes	Deposition system required; use of expensive or rare metals
Carbon Ink Off - Channel	Fair	Good	Lowest	Simple	Inexpensive	Yes	Electrode size is limited by PDMS aspect ratio; thick films can be highly resistive
Carbon Ink End - Channel	Poor	Fair	Lowest	Simple	Inexpensive	No	Electrode size is limited by PDMS aspect ratio; thick films can be highly resistive

[1] Slope of the calibration curve

[2] Calculated for S/N=3

[3] Based on average peak-to-peak baseline noise

[4] Use of HF and/or aqua regia solutions